Experimental investigation on temperature profile and pressure drop in two-phase heat exchanger for mixed refrigerant Joule–Thomson cryocooler

P.M. Ardhapurkar [a,b], Arunkumar Sridharan [a], M.D. Atrey [a,*]

[a] Mechanical Engineering Department, Indian Institute of Technology Bombay, Mumbai 400 076, India
[b] S.S.G.M. College of Engineering, Shegaon 444 203, India

HIGHLIGHTS

- Temperature distributions in a helically coiled tube-in-tube heat exchanger for MR J–T cryocooler are measured.
- The effect of mixture compositions on the temperature distributions is investigated.
- The thermal and hydraulic performances of the heat exchanger are analyzed.
- The present study finds significance in efficient design of heat exchanger for MR J–T cryocooler.

ARTICLE INFO

ABSTRACT

The heat exchanger of a mixed refrigerant Joule–Thomson (MR J–T) cryocooler forms a very important component of the cycle. The working fluid in such a heat exchanger consists of a mixture of gases which undergo condensation and boiling heat transfer simultaneously. The design of these heat exchangers, therefore, is crucial; however, heat transfer data related to such heat exchangers is not available. In the present work, temperature distributions of hot and cold fluid along the length of the helical coil heat exchanger are measured experimentally. The effect of mixture compositions on the temperature distributions in the heat exchanger is studied. The performance of the heat exchanger is analyzed in terms of overall heat transfer coefficient and the heat transfer rate. It was found that the higher values of overall heat transfer coefficient leads to decreasing cool-down time for MR J–T cryocooler. However, to achieve lower refrigeration temperatures, the greater part of the heat exchanger should experience two-phase flow and the temperature profiles should be linear. Pressure drop studies reveal that the total pressure drop for the evaporating cold stream is crucial, which strongly depends on the mixture composition and operating conditions.

© 2014 Elsevier Ltd. All rights reserved.

1. Introduction

Joule–Thomson (J–T) cryocoolers using mixed refrigerants, show a lot of promise in producing low temperatures, due to their efficiency, simple construction, operational reliability, fast cool-down time, and no electromagnetic interference. By using specific mixtures, these cryocoolers can efficiently operate in the cooling temperature range from 80 to 230 K in many applications, such as cooling infrared detectors and superconducting devices, gas chiller or liquefaction, cryosurgery, and cryo-preservation. In early 1970's, Brodyanskii et al. [1] observed that with the use of mixtures, the efficiency increased significantly as compared to nitrogen as working medium. Extensive study [2–4] shows that the use of multi-component mixtures of nitrogen-hydrocarbons in J–T refrigeration cycle can greatly improve the thermodynamic performance of the cryocooler. However, the overall performance of the cryocooler is governed by the selection of the mixture composition, the heat exchanger, and the compressor [2].

Many experimental and numerical studies have been carried out on the mixed refrigerant Joule–Thomson (MR J–T) cryocooler; however, these are mainly related to the optimization of mixtures used and the thermodynamic performance of the overall refrigeration system [1–7]. The design of the recuperative heat exchanger, used to

* Corresponding author. Tel.: +91 22 2576 7522; fax: +91 22 2572 6875.
E-mail addresses: pmardhapurkar@iitb.ac.in (P.M. Ardhapurkar), arunsri@iitb.ac.in (A. Sridharan), matrey@me.iitb.ac.in (M.D. Atrey).

pre-cool the refrigerant mixture prior to J–T expansion, is most crucial in the efficient operation of the cryocooler. However, little has been published about the heat transfer characteristics of the tubes-in-tube helical coil heat exchanger, operating with mixed refrigerants.

Gong et al. [8] reported experimental results in terms of pressure drop and temperature distribution for different operating conditions of tubes-in-tube heat exchangers with different mixtures. To measure the temperatures along the length of the heat exchanger, it was divided into segments, and temperature sensors were installed at the joints of these segments. However, it was found that this could lead to disturbance in the flow pattern and associated two-phase heat transfer characteristics in the heat exchanger. Ardhapurkar et al. [9] presented a study on the performance of the multi tubes-in-tube heat exchanger for MR J–T cryocooler. The work analyzed the effect of mixture composition on the performance of the heat exchanger, in terms of variation in overall heat transfer coefficients along the length. However, temperatures of the cold fluid were measured experimentally on the tube surface along the length of the heat exchanger while those of the hot fluid were theoretically determined using simple energy balance equations. This study did not include thermal losses and pressure drop in the heat exchanger.

Alexeev et al. [10] numerically simulated multi tubes-in-tube heat exchanger for different mixture compositions. A modified Chen correlation was used to calculate the heat transfer coefficients for forced convection, as well as for condensation of mixtures. However, the calculation results were not compared with experimental data, except for the pressure drop on the shell side. Recently, Nellis et al. [11] reported an experimental test facility and procedure that was used for the measurements of horizontal, flow boiling heat transfer coefficient. This was done for optimal nitrogen-hydrocarbon mixtures over a range of compositions, temperatures, mass flow rates and pressures, which are applicable to small scale J–T cryocoolers.

1.1. Motivation for the present work

The study of temperature and pressure profiles in the heat exchanger and their dependence on the mixture composition is crucial for the optimization of the mixture. In these heat exchangers, high pressure fluid gets condensed, while in the return line, low pressure stream gets evaporated continuously. However, there are no generalized correlations available for heat transfer by condensation and vaporization of the multi-component non-azeotropic mixtures of nitrogen-hydrocarbons. Also, no pressure drop models for the two-phase flow of such mixtures at cryogenic temperatures are available. Therefore, performance evaluation of the heat exchanger and the accurate prediction of temperature and pressure profiles in such heat exchangers are not possible, either numerically or analytically.

The objective of the present work is to analyze the performance of tube-in-tube helical coil heat exchanger. This is done by studying temperature distribution and pressure drop in the heat exchanger with respect to the composition of nitrogen-hydrocarbon multi-component mixture and operating conditions of the MR J–T cryocooler.

There is a large amount of literature published related to prediction of two-phase pressure drop. However, these empirical correlations are developed for the specific conditions and often not valid outside of these regions. Additionally, no study has yet been reported on the pressure drop behavior of multi-component mixtures of nitrogen and hydrocarbons when undergoing boiling and condensation processes. Therefore, the purpose of this paper is also to increase the basic understanding of pressure drop by presenting the experimental results using different composition of nitrogen-hydrocarbon mixtures at cryogenic temperatures.

Usually, the heat exchanger used in MR J–T cryocooler is multi tubes-in-tube helical heat exchanger in which 5 to 7 tubes of small diameters (2–5 mm) are coiled helically in a single tube. Even though it is a compact arrangement, such a heat exchanger is more difficult to fabricate compared to a simple tube-in-tube heat exchanger. Therefore, in the present study, a simple helically coiled tube-in-tube heat exchanger is used. This arrangement also facilitates the measurement of the temperature of the hot fluid circulating through the inner tube. Further, the advantages of such a heat exchanger are low axial heat conduction and a uniform flow distribution of the return line low pressure stream.
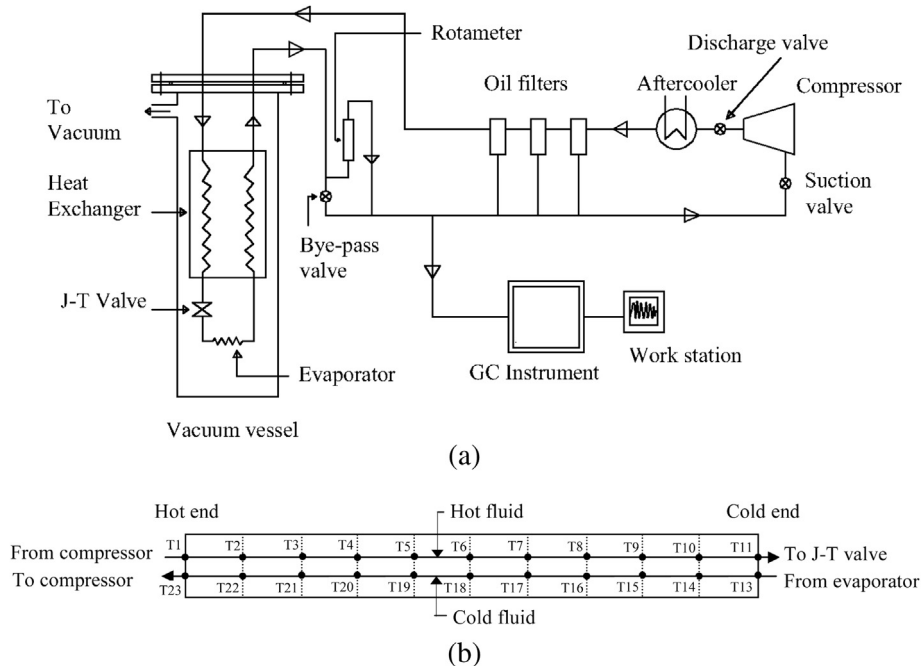

Fig. 1. (a) Experimental set-up (b) locations of sensors on heat exchanger.

Table 1
Specifications of the heat exchanger.

Tube	ID (mm)	OD (mm)
Inner	4.83	6.35
Outer	7.89	9.52

2. Experimental set-up

The experimental set-up developed in the present work is shown in Fig. 1(a). It mainly consists of a compressor, an after-cooler, oil filters, a heat exchanger, an expansion device, and an evaporator. As mentioned earlier, a simple tube-in-tube heat exchanger is used to measure the temperature distributions of both, the hot and the cold fluid. The dimensions of the helical heat exchanger are as given in Table 1. The total length of the heat exchanger is 15 m and the coil diameter is 200 mm. A capillary tube is used as an expansion device. The length and the inside diameter of the capillary tube is 2.0 m and 1.52 mm respectively. The coiled heat exchanger is as shown in Fig. 2. The heat exchanger, the capillary tube and the evaporator are placed in a stainless steel vessel in which, a vacuum of the order of 10^{-5} mbar, is maintained using a diffusion pump.

A rotameter is installed in the suction line near the compressor to measure the volume flow rate of the refrigerant at a steady state condition. The suction and the discharge pressures of the compressor are measured by two pressure gauges located at the inlet and the outlet of the compressor respectively. Pressures of the low and the high pressure stream in the heat exchanger are measured with the help of pressure gauges (Make: WIKA, Germany) with an accuracy of 0.1% full scale. The mass flow rate of the refrigerant mixture is calculated using the density of the mixture in circulation, at pressure and temperature to the inlet of rotameter. For every experiment, the composition of the mixture in circulation is measured using a gas chromatograph (Make: PerkinElmer-Clarus 500GC). The gas chromatograph instrument was calibrated with components of known purity and mixtures of known composition. All the thermodynamic properties of the mixture are calculated using Peng–Robinson equation of state [12] in aspenONE [13]. The properties of the hot and the cold fluids in the heat exchanger are evaluated for the mixture composition that is in circulation at the steady state conditions and at mean pressure of the fluid. The heat

load on the evaporator is evaluated by measuring the voltage supplied and the resultant current.

2.1. Temperature measurement

The insertion of temperature sensors into the inner tube of the heat exchanger for measuring hot fluid temperature is quite challenging. In the present work, to measure temperatures of hot fluid, a sensor belt is made by perfectly binding the sensors on one thin supporting wire using teflon tape. This ensured that the distance between any two sensors is consistently maintained. The teflon tape is wound on the entire bundle of lead wires coming out from the sensors to avoid any thermal contact in the lead wires. It also reduced the heat transfer from the hot fluid to the lead wires.

A total of eleven temperature sensors (PT100) are used to measure temperature of the hot fluid in the heat exchanger (HX–I) as shown in Fig. 1(b). Out of eleven sensors, two sensors, one at the inlet and one at the outlet of the hot fluid, T1 and T11 respectively, are installed on the outer surface of the inner tube. The remaining sensors, T2–T10, are installed on the sensor belt, and inserted into the inner tube. They measured the temperatures of the hot fluid at an interval of 1.5 m along the length of the heat exchanger. The lead wires of three wire sensors are taken out from both the ends of the tube through a tee junction so as to have a bundle of lead wires of uniform thickness, passing through the inner tube. The sensors T2–T6 (5 numbers) are taken out from the hot end of HX–I while, the remaining 4 sensors, T7–T10 are taken out from the other end of HX–I, nearer to the cold end. The outlets of both the T-connectors from where lead wires of sensors are taken out from the inner tube are filled with the low temperature epoxy (Stycast 2850) material. The lead wires are of size 33 SWG (0.254 mm) so as to have a minimum overall size. An equal number (11) of temperature sensors (T13–T23) are installed on the outside surface of the outer tube to measure return fluid temperature as shown in Fig. 1(b). One sensor (T12) is installed at the outlet of capillary to measure refrigeration temperature. All the temperature sensors are calibrated up to liquid nitrogen temperature (77 K). Temperature data at various locations is recorded using the data logging system, Data Taker-800. The temperatures of the hot and the cold fluid, recorded at the steady state are averaged over the period of minimum 10 min.

3. Theoretical analysis

In order to study the performance of the heat exchanger with respect to mixture composition, the overall heat transfer coefficient is determined using measured temperature distributions in the heat exchanger. The temperatures of the hot and the cold fluid are measured at different locations along the length of the heat exchanger. The Apparent Log Mean Temperature Difference (ALMTD) and heat transferred, q, are calculated in each section of the heat exchanger. The average LMTD for the heat exchanger is defined as given in Eq. (1).

$$\text{LMTD}_{\text{avg}} = \frac{\sum q_i}{\sum (q_i / \text{ALMTD}_i)} = \frac{h_{c2} - h_{c1}}{\sum (q_i / \text{ALMTD}_i)} \tag{1}$$

where h_{c2} and h_{c1} are enthalpies of the cold fluid at the outlet and the inlet to the heat exchanger respectively. The overall heat transfer coefficient, U_{avg}, for whole heat exchanger of area A, based on inside surface, is calculated using Eq. (2).

$$U_{\text{avg}} = \frac{\dot{Q}_{\text{total}}}{A(\text{LMTD})_{\text{avg}}} = \frac{\dot{m}(h_{c2} - h_{c1})}{A(\text{LMTD})_{\text{avg}}} \tag{2}$$

Fig. 2. Pictorial view of helical heat exchanger.

Table 2
Uncertainty analysis.

Parameter	Uncertainty		
	Mix#1	Mix#2	Mix#3
Temperature	±0.59−0.62 °C	±0.59−0.65 °C	±0.59−0.63 °C
Mass flow rate	±1.66%	±1.66%	±2%
Pressure	±1.6%	±1.6%	±1.6%
ALMTD	4.82−12.0%	3.10−12.53%	3.52−28.75%
Heat transfer rate	±0.43%	±0.45%	±0.75%
Overall HTC	4.84−12.0%	3.14−12.54%	3.6−28.76%

4. Experimental uncertainty

The uncertainties in the experimental data are calculated using root-sum-square (RSS) method suggested by Kline and McClintock [14]. If the result, R, is a function of n independent variables x_1, x_2, x_3, …x_n and w_1, w_2, w_3, ….w_n are the uncertainties in the independent variables then the uncertainty in the result, R, is calculated as given in Eq. (3).

$$W_R = \left[\left(\frac{\partial R}{\partial x_1} w_1 \right)^2 + \left(\frac{\partial R}{\partial x_2} w_2 \right)^2 + \dots + \left(\frac{\partial R}{\partial x_n} w_n \right)^2 \right]^{1/2} \quad (3)$$

The uncertainties for all the temperature sensors are obtained from combining systematic and random uncertainties assuming student's t-distribution with 95% confidence level. Table 2 summarizes the results of the uncertainty analysis carried out for all the experiments conducted. The expanded uncertainties in the temperatures vary in the range of ±0.59 to ±0.65 °C. The uncertainties propagated in ALMTD are in the range of 3.1−28.75% for all the mixtures. It is noted that the uncertainties in ALMTD and overall heat transfer coefficient are nearly same and are more, where the nominal values of temperature difference between the hot and the cold fluid are less. These uncertainties mainly resulted from measurement error of the temperature sensors.

5. Results and discussion

Experiments are conducted with various mixture compositions which are designed to generate specific cases of temperature distributions, in the heat exchanger with regards to pinch point. In the present case, the pinch point is defined to have occurred when the temperature difference between the hot and the cold fluid is less than 5 K. These mixture compositions also yield different low temperatures. The test conducted on each mixture is repeated at least three times to ensure repeatability of the results obtained. Three specific compositions of the mixture of gases viz. nitrogen, methane, ethane, propane and iso-butane are used as a refrigerant in the system. Gong et al. [15] observed a composition shift of the mixture in circulation. In the present work also, it is noticed that the composition of the mixture in circulation is different from the one which is charged. Table 3 gives the composition, of the mixture charged, and of that in circulation, corresponding to each range of refrigeration temperature. The composition of Mix#1 is selected in

such a way so as to reach temperature in the range of 140−150 K. Mix#1 has lower percentage of high boiling point components (propane and iso-butane) and higher composition of middle boiling point component (i.e. ethane) than that of Mix#2 and Mix#3. Mix#2 and Mix#3 are designed so that these consist of nearly the same composition of high boiling point components (propane and iso-butane), and is more than that for Mix#1. However, Mix#2 consists of larger percentage of low boiling component, nitrogen, than Mix#3 and is optimized to get lower refrigeration temperature. The details regarding operating conditions like mass flow rates, refrigeration temperatures, pressures at the inlet and the outlet to the heat exchanger for both, the hot and the cold fluids, are given in Table 4. The no load refrigeration temperature, T_{low}, obtained is 143.98 K and 113.45 K for Mix#1 and Mix#3 respectively, whereas it is the lowest for Mix#2, at 98.62 K.

5.1. Effect of inside sensors and leads on temperature measurement

In order to obtain reliable performance of the heat exchanger, tests are conducted to investigate the effect of physical existence of the temperature sensors and their leads on the hot fluid temperature measurement inside the inner tube. For this purpose, another heat exchanger, HX−II, of the same dimensions as HX−I, is fabricated. However, the temperature sensors, T2−T10, are not inserted in the inner tube, which are meant for the hot fluid. The only temperatures, those are measured of the hot fluid, are at the inlet and the outlet of HX−II. The temperatures of the cold fluid are measured by the sensors T13−T23, installed on the outside surface of the outer tube similar to HX−I. Experiments are carried on these heat exchangers, keeping the same operating pressures and mass flow rates for all the mixture compositions.

It is observed from the tests that there is no significant difference in the temperature profile of the cold fluid and refrigeration temperature produced using HX−I and HX−II. The low temperatures obtained for HX−I (with inside sensors) and HX−II (without inside sensors) are 113.45 K and 115.34 K respectively, for Mix#3. The pressure drop for hot fluid is 0.7 bar in case of HX−I, while for HX−II, it is 0.65 bar. The results for other mixtures show similar results with HX−I and HX−II. In view of this, it may be concluded that the effect of physical existence of the sensors on heat transfer phenomenon could be neglected. Therefore, further experiments are conducted on HX−I in order to study the temperature profiles and pressure drop for various mixtures.

5.2. Thermal performance of heat exchanger

Fig. 3 shows the temperature distributions in HX−I for Mix#1 without heat load. It is clear from Fig. 3 that the pinch points occur, both at the cold end, and nearer to the hot end of the heat exchanger. This is due to the lower percentage of nitrogen and propane in Mix#1. Table 5 gives the bubble point temperature, T_{bub}, the dew point temperature, T_{dew}, and temperature glide, ΔT_g, of the hot and the cold fluid for all the mixtures. These temperatures are evaluated at mean pressures of the fluids using the software − aspenONE [13]. It is noted from Fig. 3 that the hot fluid leaves the

Table 3
Mixture specifications.

Mixture	Mixture composition, $N_2/CH_4/C_2H_6/C_3H_8/iC_4H_{10}$ (% mol)		Temperature range (K)
	Charged	Circulation	
Mix#1	5.5/42.5/36.0/5.0/11.0	6.99/46.335/33.533/3.996/9.146	140−150
Mix#2	36.0/15.0/13.0/19.0/17.0	39.86/16.865/12.845/17.38/13.045	<100
Mix#3	15.5/31.0/16.5/21.0/16.0	18.455/32.785/16.05/20.14/12.57	110−120

Table 4
Operating conditions for different mixtures used.

| Mixture	Heat load	T_{low}, (K)	Mass flow rate, (g/s)	$P_{h,in}$, (bar)	$P_{h,out}$, (bar)	$(\Delta P)_h$	% $(\Delta P)_h$	$P_{c,in}$, (bar)	$P_{c,out,}$ (bar)	$(\Delta P)_c$	% $(\Delta P)_c$
Mix#1	No load	143.98	3.8	12.38	11.41	0.97	7.83	6.11	3.21	2.9	47.46
	5 W	145.82	3.8	12.87	11.89	0.98	7.61	6.11	3.21	2.9	47.46
Mix#2	No load	98.62	3.7	14.74	13.95	0.79	5.36	5.61	2.61	3.0	53.47
	5 W	102.13	3.6	15.08	14.35	0.73	4.84	5.57	2.51	3.0	54.93
Mix#3	No load	113.45	2.64	11.7	11.01	0.69	5.89	5.57	2.31	3.26	58.52
	5 W	116.49	2.6	12.28	11.61	0.67	5.45	5.32	2.31	3.0	56.39
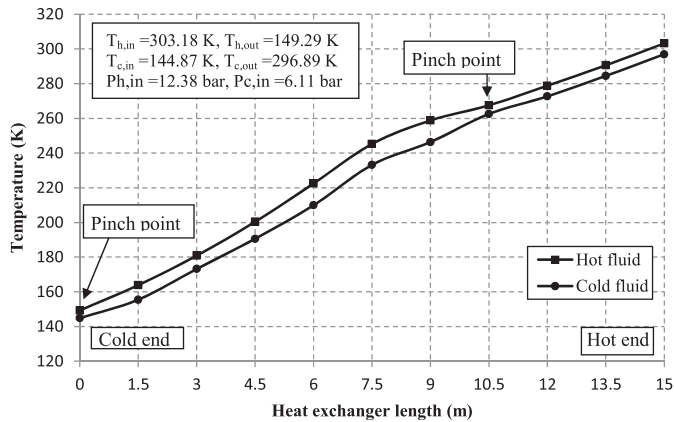
Fig. 3. Temperature profiles for Mix#1.

heat exchanger at 149.29 K which is greater than its bubble point temperature. Similarly, the cold fluid enters the heat exchanger at 144.87 K, which is also greater than its bubble point temperature. This means that the hot fluid changes its state from gas to two-phase region while the return line cold stream changes its state from two-phase to gas region at their respective dew point temperatures. This may be noticed from the change of slope of the temperature profiles at 267 K and 246 K temperature locations, for the high pressure and the low pressure streams respectively.

The variations in temperature difference (ALMTD), heat transfer rate (Q) and overall heat transfer coefficient (HTC) for Mix#1 are shown in Fig. 4. From this figure, it is obvious that the temperature difference between the hot and the cold fluid is non-uniform along the length of the heat exchanger and pinch points occur at certain locations. The variation in the temperature difference is mainly due to non-linear variation of enthalpies of the multi-component non-azeotropic mixture flowing at different pressures in the heat exchanger. This may be explained that the temperature distribution in the heat exchanger depend on variation of specific heat of the mixture. The heat capacity rate is a complex function of temperature, pressure and composition of the mixture. The heat capacity rate ratio, c, is defined as the ratio of heat capacity rate of the hot fluid to that of the cold fluid. The variation in heat capacity rate ratio with respect to temperature is plotted for all the mixtures studied, and is shown in Fig. 5.

It is noticed from Figs. 3 and 4 that the temperature profiles are linear and the temperature difference between the two fluids is

Table 5
Temperature glides for mixtures.

Mixture	Hot fluid temperature, K			Cold fluid temperature, K		
	T_{bub}	T_{dew}	ΔT_g	T_{bub}	T_{dew}	ΔT_g
Mix#1	139.29	267.64	128.35	114.62	245.46	130.84
Mix#2	103.61	287.15	183.54	86.74	253.77	167.03
Mix#3	110.97	281.79	170.82	92.42	253.56	161.14

nearly constant at the hot end of the heat exchanger. This is due to the fact that both the streams are in single phase vapor state, and have equal heat capacities ($c = 1$), as evident from Fig. 5. As the hot fluid begins to condense, the temperature difference between the two fluids increases due to sudden increase in the specific heat of the hot fluid at its dew point temperature, and heat capacity rate ratio increases to maximum, i.e. $c = 3.5$. The maximum temperature difference (ALMTD) is noted to be 12.3 K at the middle section of the heat exchanger where both the streams undergo change of phase. The temperature difference decreases towards the cold end of the heat exchanger due to decrease in the specific heat capacity of the hot fluid and increase in the specific heat capacity of the cold fluid. At the cold end, the specific heat of the cold fluid is greater than that of the hot fluid, which minimizes the temperature difference. The ratio of heat capacity rates of the hot and the cold streams is found to be 0.61 at 145 K ($c < 1$). It is also clear from Fig. 3 that the slope of the temperature profile of the cold fluid is relatively less at the cold end up to 1.5 m section of the heat exchanger.

The variation in temperatures of the hot and the cold fluid affects the performance of the heat exchanger. It can be observed from Fig. 4 that the heat transfer rate at the hot end of the heat exchanger, where both the fluids are in single phase, is relatively lower because of lower values of the overall HTC and the temperature difference between the two fluids. The heat transfer rate is found to be minimum (67 W) at the location of the pinch point, which occurs in the single phase region nearer to the hot end. The overall HTC increases in the region of phase change where, both the hot and the cold fluid get progressively condensed and evaporated respectively. The increase in overall HTC and ALMTD leads to increase in heat transfer rate in the region of phase change and it is found to be maximum at the middle section of the heat exchanger. Heat transfer rate decreases from the middle section towards the cold end of the heat exchanger due to decrease in temperature difference and overall HTC.

Fig. 6 gives the steady state temperature profiles of the hot and the cold fluid for Mix#2, which has pinch point at the middle of the
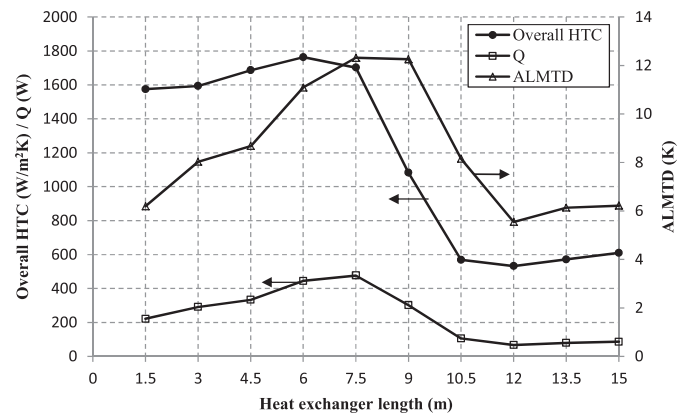

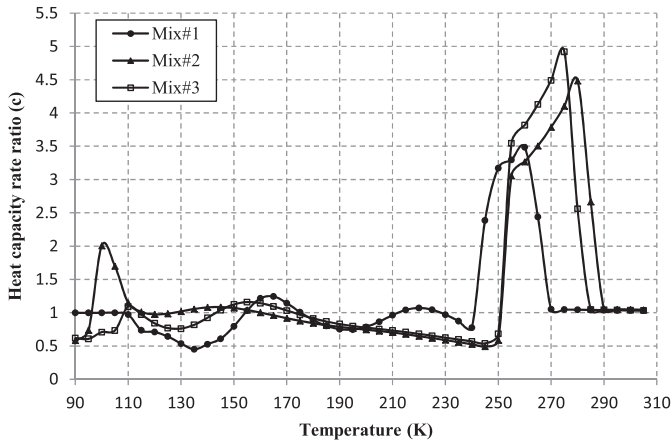**Fig. 4.** Variation of overall HTC, Q and ALMTD for Mix#1.

Fig. 5. Variation of specific heat capacity rate ratio for Mix#1, Mix#2 and Mix#3.

Fig. 7. Variation of overall HTC, Q and ALMTD for Mix#2.

heat exchanger. This is due to relatively low percentage of middle boiling point component, i.e., ethane in the overall composition of the mixture. The temperature difference between the hot and the cold fluids at the cold end for Mix#2, is more than that for Mix#1 due to higher percentage of the low boiling components in Mix#2. The higher percentage of low boiling point components also results in lower refrigeration temperature, below 100 K. The hot fluid leaves the heat exchanger at 110.53 K whereas the cold fluid enters the heat exchanger at 100.17 K. Temperature glide for the hot and the cold fluid for Mix#2 is more than that for Mix#1, as seen from Table 5. This indicates that two-phase region for both, high and low pressure streams is more in Mix#2 as compared to the one for Mix#1. It is also observed from Fig. 6 that the temperature profiles are almost linear in the two-phase region of the heat exchanger for Mix#2.

Fig. 7 shows the variations in the ALMTD, Q and overall HTC for Mix#2. It is found from Figs. 6 and 7 that the temperature difference is more at the hot end, and in the region of the phase change of the heat exchanger, due to higher percentage of high boiling point components in the Mix#2. It is noted that the maximum temperature difference (ALMTD) is around 20 K at the distance of 12 m from the cold end. Beyond this location, temperature difference between the two fluids decreases towards the two-phase region of the heat exchanger similar to that in Mix#1, because of variation in specific heats, as shown in Fig. 5. However, the temperature difference in the two-phase region is relatively less in the case of Mix#2 than that of Mix#1. It is nearly constant from middle section
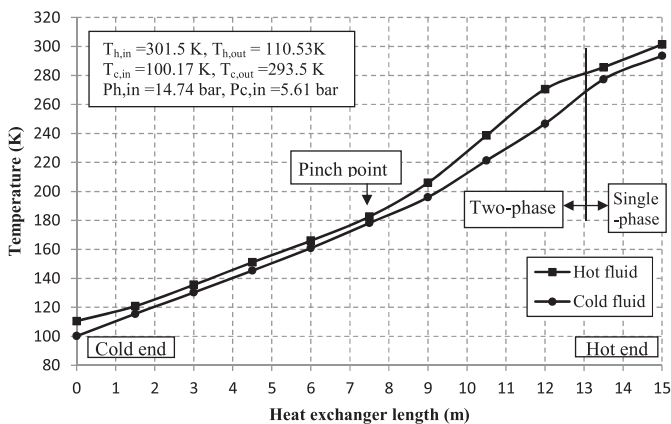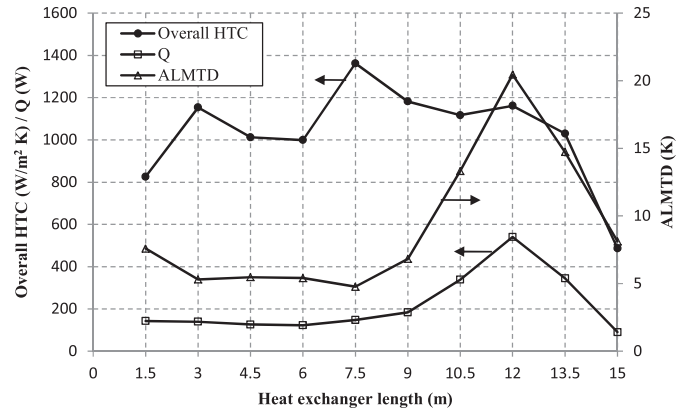
towards the cold end, up to 1.5 m length of the heat exchanger. In the region where both the fluids are in two-phase state, specific heat of the cold fluid is greater than that of the hot fluid ($c < 1$), and the difference between two heat capacities decreases towards the cold end. At the cold end, heat capacity rate ratio becomes more than one ($c = 2.0$) at temperature of 100 K. This also explains the reason for increase in the temperature difference at the cold end.

It may also be observed from Fig. 7, that the heat transfer rate increases from the hot end of the heat exchanger for Mix#2 due to immediate increase in the temperature difference. This is in contrast to Mix#1, since the single phase region for Mix#2 is smaller at the hot end as compared to Mix#1. The heat transfer rate is found to be maximum at the location of phase change of the hot fluid due to higher value of ALMTD. The heat transfer decreases in the region of phase change up to the middle section of the heat exchanger. This is due to decrease in ALMTD, even though the overall HTC increases. However, in the two-phase region, which is in the middle section of the heat exchanger, the heat transfer rate remains almost constant. This indicates that the effect ALMTD has, on the heat transfer rate is more prominent than the overall HTC.

The temperature profiles for no load condition are shown in Fig. 8 for Mix#3. It is obvious from the figure that the temperature difference is minimum at the cold end of the heat exchanger. The pinch point in this case, occurs at the cold end of the heat exchanger because of less molar percentage of low boiling point component, nitrogen, in Mix#3. It can be noted from Table 5 and from the inlet conditions of the fluids, that the two-phase region of both the streams is maximum for Mix#2 and minimum for Mix#1.

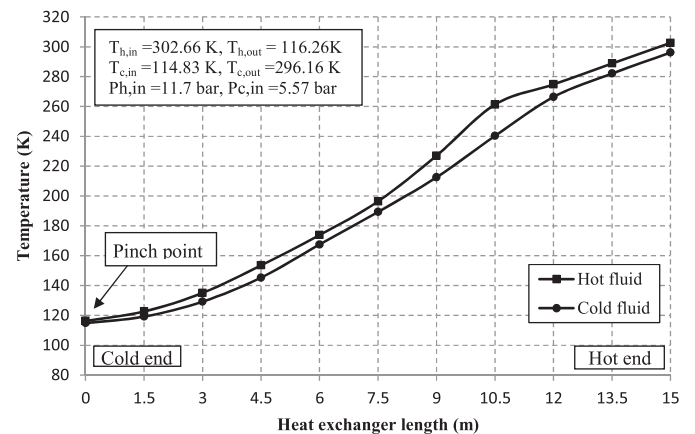Fig. 6. Temperature profiles for Mix#2.

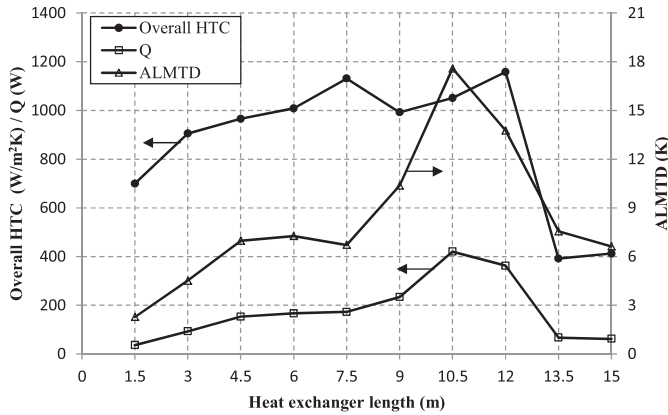Fig. 8. Temperature profiles for Mix#3.

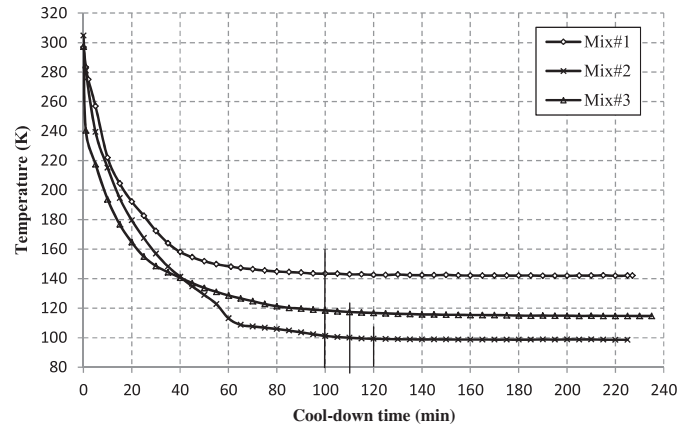Fig. 9. Variation of overall HTC, Q and ALMTD for Mix#3.

Fig. 10. Cool-down curves for Mix#1, Mix#2 and Mix#3.

It may also be noticed that the temperature profiles for Mix#3 are non-linear in the region of two-phase in contrast to Mix#2. From Fig. 8, it may be seen that the slope of temperature profiles is less at the cold end as compared to those for Mix#1 and Mix#2. This indicates that for this case the percentage of liquid fraction is more at refrigeration temperature than that for the other two mixtures. This is also evident from the fact that for Mix#3, the increase in refrigeration temperature with heat load is less due to increase in latent heat.

Fig. 9 gives the variation in ALMTD, Q and the overall HTC across the length of the heat exchanger for Mix#3. The ALMTD increases from the hot end of the heat exchanger reaching a maximum value of around 17.6 K in the region of phase change, and decreases up to middle section of the heat exchanger similar to that in Mix#2. However, the temperature difference is found to be non-uniform in the two-phase region due to variations in the ratio of heat capacity. Fig. 5 gives the variation in ratio of heat capacities of the two streams for Mix#3 in comparison to Mix#1 and Mix#2. The overall HTC coefficient varies in a non-linear manner in the two-phase region. Also, the local values of the overall HTC coefficients along the length of the heat exchanger are less for Mix#3 compared to those for Mix#1 and Mix#2. It may be noticed that the trend in variation of the heat transfer rate is similar to that in Mix#1. It decreases from the middle section towards the cold end of the heat exchanger, mainly due to variation in temperature difference. The heat transfer rate is found to be the lowest (36 W) in Mix#3 at the location of pinch point at the cold end. This limits the refrigeration temperature to above 110 K only.

The average values of LMTD, Q and overall HTC of the heat exchanger for the mixtures studied, are compared in Table 6. It is found that the average LMTD is nearly same for all the mixtures whereas heat transfer rate and average overall HTC for Mix#1 is more than that for Mix#2 and Mix#3. In order to analyze the effect of performance of the heat exchanger on MR J–T cryocooler, cool-down curves for all the mixtures are plotted. The cool-down curve indicates the time required to produce the steady state refrigeration temperature of any cryocooler and is a plot of temperature variation versus time. Fig. 10 gives the comparison of the cool-down

curves for all the mixtures studied. It is revealed that the cool-down time for Mix#1 is the lowest, around 100 min, since the heat transfer rate is the maximum for Mix#1. Mix#2 and Mix#3 need more than 110 and 120 min respectively to reach steady state.

5.3. Effect of heat load on the temperature distribution

The effects of heat load on the temperature distribution and the performance of the heat exchanger are studied for all the mixtures considered in the present work. However, on a representative basis, results are presented for Mix#1 only. Fig. 11 shows temperature profiles of the hot and the cold fluid for Mix#1 with applied heat load of 5 W. It is observed from Fig. 11 that the temperature profiles get shifted to a higher level with the heat load; however the overall trend of the temperature profiles remains the same. The increased temperatures of the hot and the cold fluids at the inlet and the outlet to the heat exchanger with 5 W heat load are compared with the no load conditions for Mix#1, as shown in Table 7. The refrigeration temperature increases from 143.98 K to 145.82 K at heat load of 5 W. Similarly, there is an increase in refrigeration temperature for the other two mixtures with the heat load applied, as shown in Table 4. It is also noted from Table 4 that the mass flow rate remains same for Mix#1, with and without heat load; whereas, there is a little decrease in mass flow rate for Mix#2 and Mix#3 with heat load compared to no load. The variations in ALMTD, Q and overall HTC are shown in Fig. 12. It is noted that the heat transfer rate increases due to increase in overall HTC with the heat load.
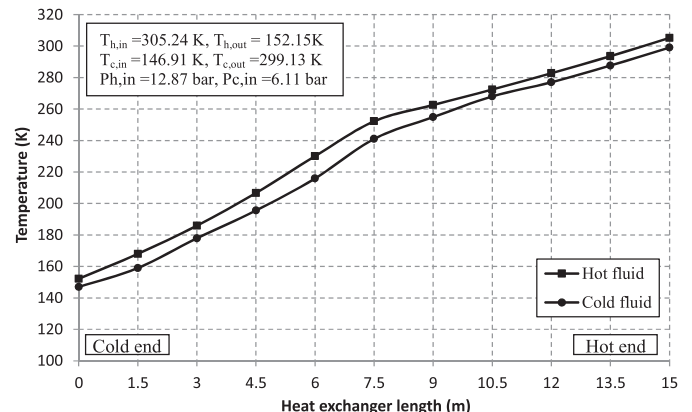
Table 6
Average LMTD and overall heat transfer coefficients for the mixtures.

Mixture	Average LMTD (K)	Heat transfer rate, $\dot{Q}_{total}$ (W)	Overall HTC, U_{avg} (W/m^2 K)
Mix#1	9.06	2408.4	1168.75
Mix#2	9.26	2176.45	1033.13
Mix#3	8.92	1768.25	871.36

Fig. 11. Temperature profiles for Mix#1 with heat load of 5 W.

Table 7
Effect of heat load on the temperatures in the heat exchanger for Mix#1.

Location	Condition	Temperature (K)	
		Hot fluid	Cold fluid
Inlet	No load	303.18	144.87
	5 W	305.24	146.92
Outlet	No load	149.29	296.89
	5 W	152.15	299.13

Table 8
Density and mass vapor fraction of cold fluid at inlet conditions to the heat exchanger.

Mixture	Liquid density, (ρ_l), kg/m^3	Vapor density, (ρ_v), kg/m^3	Density ratio, (ρ_l/ρ_v)	Mass vapor fraction
Mix#1	552.31	11.285	48.939	0.13008
Mix#2	672.699	21.4716	31.329	0.275
Mix#3	626.729	17.0737	36.70	0.12573

It may be noted from the results discussed above, for the three different cases of the mixture that the performance of the heat exchanger depends strongly on the composition of the mixture. The mixture with low fraction of a certain component will have pinch point at the temperature range corresponding to its boiling point temperature. On the contrary, if the certain component is more in the mixture, the temperature difference between the two fluids, increases at the location of boiling point of that component in the heat exchanger. The occurrence of pinch point in the heat exchanger deteriorates the performance of the heat exchanger. The enthalpies of the mixture in circulation vary non-linearly, particularly in the two-phase region. This results in a non-linear variation in the temperature profiles across the heat exchanger length. Therefore, it is important to optimize the mixture composition to have linear temperature profiles in the two-phase region of the heat exchanger. Also, the temperature difference between the hot and the cold fluid should be optimum and constant.

5.4. Hydraulic performance of the heat exchanger

Table 4 gives the measured pressure drop for the hot and the cold fluids in all the three cases of mixtures studied in the present work. The measured pressure drop includes both, the two-phase pressure drop of the evaporating or the condensing stream, and pressure drop for single phase. It is seen from Table 4 that the percentage drop in pressure (based on inlet pressure) is higher for the cold fluid, (ΔP_c) than that for the hot fluid, (ΔP_h) for all the mixtures. The percentage drop in pressure for the hot fluid varies in the range of 5–8%, while it is 47–59% for the cold fluid. This is due to an increase in kinetic energy of the cold fluid during boiling process which increases the momentum pressure drop leading to increase in total pressure drop. Additionally, mass flux of the cold fluid is marginally higher in comparison to that of the hot fluid. For the hot fluid, on the contrary, there is some recovery of pressure loss during condensation in the heat exchanger, which results in lowering of total pressure drop. The change in pressure drop of the mixture between no load and 5 W heat load case is found to

Fig. 12. Variation of overall HTC, Q and ALMTD for Mix#2 with heat load of 5 W.

be insignificant due to small increase in the refrigeration temperatures.

The relative variation in the total pressure drop of the evaporating cold fluid for the different mixtures can be explained on the basis of fundamental understanding of the two-phase flow. In general, the two-phase frictional pressure drop is due to interaction between the liquid and the vapor phase. Relative velocities between vapor and liquid phase, which depend on the respective densities of the phases, play an important role in two-phase frictional loss in pressure. Higher vapor density corresponds to lower pressure drop due to lower relative vapor velocities. The properties of the nitrogen-hydrocarbon mixed refrigerants depend on the composition of the mixture. The liquid and the vapor density of the mixture change with respect to its composition, saturation temperature and pressure. Additionally, two-phase pressure drop is a function of mass flux and quality (mass vapor fraction) of the mixture. Table 8 gives density ratio (ratio of liquid to vapor density) and mass vapor fraction of the evaporating cold fluid at the inlet condition to the heat exchanger for all the mixtures.

It is observed from Table 4 that the percentage drop in pressure for the cold fluid, ($\Delta P)_c$, of Mix#1 is lower than that for the cold fluid of Mix#2 and Mix#3. In spite of almost the same mass flow rates for Mix#1 and Mix#2, and higher density ratio for Mix#1 than that for Mix#2, the total pressure drop in the cold fluid for Mix#1, is less than that for the Mix#2. This is due to the fact that the two-phase region of the heat exchanger for Mix#1 is less (about 9 m) than that for Mix#2 (about 12 m), as seen from Figs. 5 and 6 respectively. The length of the heat exchanger for which the cold fluid experiences a two-phase flow depends mainly on its dew point temperature and its temperature at the inlet to the heat exchanger, which is ultimately a function of temperature glide of the mixture. It is found that the temperature difference between dew point temperature and temperature of the cold fluid at the inlet to heat exchanger for Mix#2 is 153.6 K, whereas it is 100.6 K only for Mix#1. Usually, the two-phase pressure drop of evaporating fluid is greater than the pressure drop of vapor phase for the same mass flux.

The temperature difference between dew point temperature and the temperature of cold fluid at the inlet to heat exchanger for Mix#3 is 138.74 K, which is more than that for Mix#1. Therefore, for Mix#3, the greater part of the heat exchanger on the cold side remains in two-phase, compared to that for Mix#1. Hence, the total pressure drop of the cold fluid for the Mix#3 is more than that for Mix#1, even though Mix#3 has low mass flow rate than Mix#1. The mass vapor fractions of the cold fluid at the inlet to the heat exchanger for Mix#1 and Mix#3 are nearly same, whereas, it is more for the Mix#2 as seen in Table 8. It can also be noted from Table 8 that the density ratio for Mix#3 is more than that for Mix#2. Therefore, pressure drop in the cold fluid for Mix#3 is more than that for Mix#2.

From the above study, it can be concluded that the pressure drop in the evaporating mixtures at low pressures, depends on the mixture composition and its properties such as bubble point and dew point temperature, in addition to the density ratio, mass flux and quality. Analysis of the total pressure drop, measured for the condensing hot stream in the heat exchanger, is difficult since the
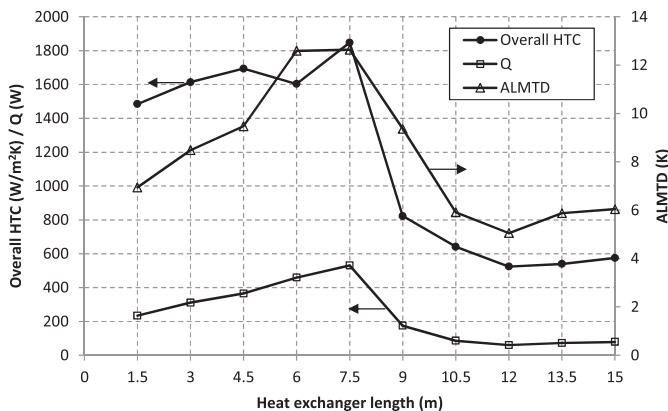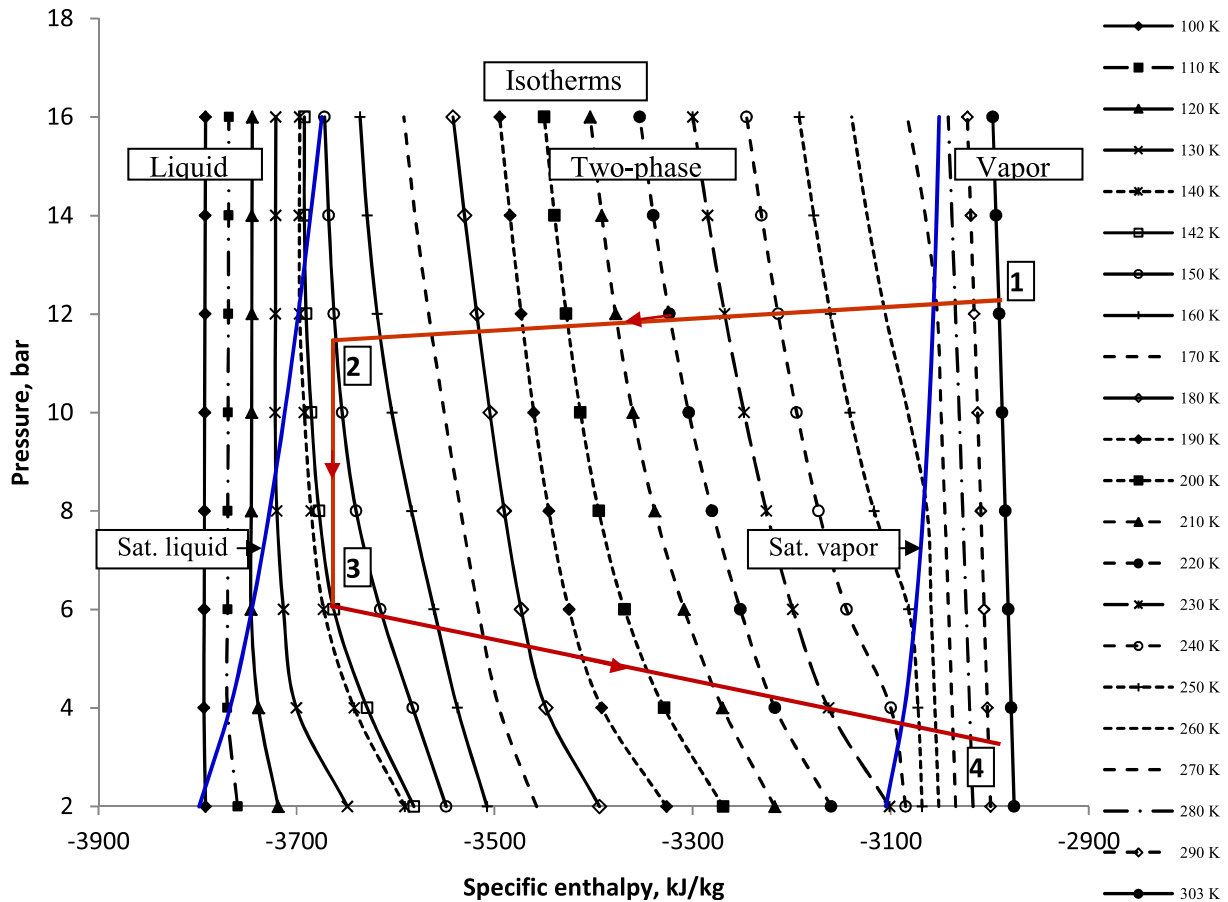
Fig. 13. *P–h* diagram for Mix#1.

location of start of two-phase flow and inlet pressure for condensation is unknown.

5.5. Verification of property data using P–h chart

Fig. 13 shows the P-h chart for Mix#1 with the cycle operating at no load condition. Enthalpies of Mix#1 are obtained from the software aspenONE [13]. Isotherms ranging from 100 K to 303 K are also shown on the P-h chart. Points 1 and 2 shown on the P-h chart indicate the actual state of the hot fluid entering and leaving the heat exchanger respectively. It is evident from the figure that point 2 lies in the two-phase region, close to the saturated liquid line, which indicates that the complete condensation of the hot fluid does not take place in the heat exchanger. It means that the surface area of the heat exchanger is insufficient to achieve lower refrigeration temperature for Mix#1.

The process 2–3 is an isenthalpic expansion. The state of the mixture leaving the expansion device, i.e. point 3, is obtained by intersection of isenthalpic line with the measured pressure of the cold fluid entering the heat exchanger. The temperature of the mixture after expansion corresponding to the point 3, noted from the P-h chart, is found to be around 142 K. The measured value of the temperature after expansion is noted to be 143.98 K. The difference in the temperatures obtained using P-h chart, and by measurement is not significant. This confirms the validity of the use of property data obtained from the aspenONE [13] against the experimental results. The process 3–4 refers to the evaporation of the cold fluid in the heat exchanger. Fig. 13 also reveals the fact that there is a significant temperature variation during phase change, particularly for

the nitrogen-hydrocarbon mixtures. The mixture at state 4 enters the compressor. However, the compression process and the heat exchange in the after-cooler are not shown on the P-h chart.

6. Conclusions

In the present study, temperature distributions for both the hot and the cold fluid in the tube-in-tube helical heat exchanger used in mixed refrigerant J–T cryocooler are determined experimentally. This work is significant due to the fact that very few experimental results are available in the literature, which explains performance of such heat exchanger. Additionally, temperature and pressure profiles cannot be predicted due to lack of accurate heat transfer and pressure drop models, for such heat exchangers operating with multicomponent non-azeotropic mixtures at cryogenic temperatures.

Experiments are conducted on the heat exchanger with three different multi-component mixtures of nitrogen-hydrocarbons to analyze its performance in terms of overall heat transfer coefficient and heat transfer rate. The study revealed that

1. The temperature distribution in the heat exchanger depends on the mixture composition and their properties. The occurrence of pinch point in the heat exchanger deteriorates the performance of the heat exchanger.
2. The average overall heat transfer coefficients vary in the range of 871 W/m² K to 1169 W/m² K for the operating conditions of the present work. Cool-down time of the cryocooler would be less for the mixture with higher value of overall heat transfer coefficient.

3. The pressure drop as a percentage of inlet pressure in the hot fluid varies in the range of 5−8% for the three mixtures, while it is 47−59% in the cold fluid for the present heat exchanger. The inlet pressure in case of the hot fluid is in the range of 12−15 bar, while it is much lower in the range of 5−6 bar for the cold fluid. A comparison across the mixture for the cold fluid reveals that ΔT_g for Mix#2 is greater than that for Mix#1; therefore, pressure drop in the cold fluid for Mix#2 is more than that for Mix#1. Similarly, ΔT_g for Mix#3 is greater than that for Mix#1; therefore, pressure drop in the cold fluid for Mix#3 is more than that for Mix#1. It is noticed that the pressure drop varies with respect to mixture composition; it increases with the increase in temperature glide of the mixture in the heat exchanger.

It can be concluded that the refrigeration temperature and the cooling capacity of the mixed refrigerant J−T cryocooler strongly depend on the mixture composition and the performance of the heat exchanger. The results of the experimental investigation are useful for the design of a highly efficient heat exchanger for mixed refrigerant J−T cryocooler.

Nomenclature

A	inside surface area of the heat exchanger, m^2
ALMTD	apparent logarithmic mean temperature difference, K
c	ratio of heat capacity rate of hot fluid to cold fluid
h	enthalpy, kJ/kg
HTC	heat transfer coefficient, W/m^2 K
HX	heat exchanger
ID	inner diameter, mm
LMTD	logarithmic mean temperature difference, K
$\dot{m}$	mass flow rate, kg/s
Mix#1	mixture 1
Mix#2	mixture 2
Mix#3	mixture 3
OD	outer diameter, mm
P	pressure, bar
q	specific enthalpy difference, kJ/kg
$\dot{Q}$	heat transfer rate, W
T	temperature, K
T_{low}	refrigeration temperature, K
U	overall heat transfer coefficient, W/m^2 K
ΔP	pressure drop, bar
ΔT	temperature difference, K
ρ	density, kg/m^3

Subscripts

avg	average
bub	bubble point
c	cold fluid
dew	dew point
g	glide
h	hot fluid
i	ith section in heat exchanger
l	liquid
total	total
v	vapor
1, in	inlet
2, out	outlet

References

[1] V.M. Brodyanskii, E.A. Gromov, A.K. Grezin, V.M. Yagodin, V.A. Nikolaskii, A.G. Tashchina, Efficient throttling cryogenic refrigerators which operate on mixtures, Chem. Pet. Eng. 7 (12) (1971) 1057−1061.

[2] R.C. Longsworth, M.J. Boiarski, L.A. Klusmier, 80 K closed cycle throttle refrigerator, Cryocoolers 8 (1995) 537−541.

[3] N.S. Walimbe, K.G. Narayankhedkar, M.D. Atrey, Experimental investigation on mixed refrigerant Joule−Thomson cryocooler with flammable and non-flammable refrigerant mixtures, Cryogenics 50 (10) (2010) 653−659.

[4] A. Alexeev, Ch. Haberstroh, H. Quack, Further development of a mixed gas Joule Thomson refrigerator, Adv. Cryog. Eng. 43 (1998) 1667−1674.

[5] F. Keppler, G. Nellis, S.A. Klein, Optimization of the composition of a Gas mixture in a Joule−Thomson cycle, HVACR Res. 10 (2) (2004) 213−230.

[6] M.Q. Gong, E.C. Luo, Y. Zhou, J.T. Liang, L. Zhang, Optimum composition calculation for multicomponent cryogenic mixture used in Joule−Thomson refrigerators, Adv. Cryog. Eng. 45 (2000) 283−290.

[7] N. Lakshmi Narasimhan, G. Venkatarathnam, Effect of mixture composition and hardware on the performance of a single stage JT refrigerator, Cryogenics 51 (8) (2011) 446−451.

[8] M.Q. Gong, J.F. Wu, E.C. Luo, Y.F. Qi, Q.G. Hu, Y. Zhou, Study on the overall heat transfer coefficient for the tube-in-tube heat exchanger used in mixed-gases coolers, Adv. Cryog. Eng. 47B (2002) 1483−1490.

[9] P.M. Ardhapurkar, A. Sridharan, M.D. Atrey, Investigations on two-phase heat exchanger for mixed refrigerant Joule−Thomson cryocooler, Adv. Cryog. Eng. 57A (2012) 706−713.

[10] A. Alexeev, A. Thiel, Ch. Haberstroh, H. Quack, Study of behavior in the heat exchanger of a mixed gas Joule−Thomson cooler, Adv. Cryog. Eng. 45 (2000) 307−314.

[11] G. Nellis, C. Hughes, J. Pfotenhauer, Heat transfer coefficient measurements for mixed gas working fluids at cryogenic temperatures, Cryogenics 45 (8) (2005) 546−556.

[12] D. Peng, D.B. Robinson, A new two-constant equation of state, Ind. Eng. Chem. Fundam. 15 (1) (1976) 59−64.

[13] aspenONE, V 7.1, Aspen Technology, Inc., Burlington, MA 01803, USA, 2009.

[14] S.J. Kline, F.A. McClintock, Describing uncertainties in single-sample experiments, Mech. Eng. 75 (1953) 3−8.

[15] M.Q. Gong, J.F. Wu, E.C. Luo, Y.F. Qi, Q.G. Hu, Y. Zhou, Research on the change of mixture compositions in mixed-refrigerant Joule−Thomson cryocoolers, Adv. Cryog. Eng. 47A (2002) 881−886.